Solid-State High-Resolution ^{13}C NMR Studies on the Structure–Property Relationship of Simultaneous Interpenetrating Networks from Castor Oil Based Polyurethane and Polystyrene

Wen-Hsiung Ku, Jeng-Li Liang, Kuo-Tung Wei, and Hsin-Tzu Liu

The Chemical System Research Division, Chun Shan Institute of Science and Technology, P.O. Box 90008-17-13, Lung-Tan, Taiwan 32526, R.O.C.

Chung-Shing Huang, Suh-Yun Fang, and Wen-guey Wu*

Institute of Life Sciences, National Tsing Hua University, Hsinchu, Taiwan 30043, R.O.C.

Received November 19, 1990; Revised Manuscript Received January 4, 1991

ABSTRACT: Cross-polarization/magic angle spinning ^{13}C nuclear magnetic resonance (NMR) was applied to reveal the microphase structures and the structure–property relationship of simultaneous interpenetrating networks (SINs) from castor oil–polyurethane and polystyrene. First, the size of the microphase structures (~100 Å) estimated by NMR proton spin diffusion is 2–3 orders magnitude smaller than the domain (0.1–1 μm) observed by the electron microscopic method. Therefore, a high degree of heterogeneity is present in the macroscopic domain. At the macroscopic level, both Young's modulus–composition data and scanning electron microscopic measurements showed the occurrence of phase inversion at 20–30 wt % polyurethane composition. At the molecular level, however, the phenyl rotation of polystyrene as revealed by the line width of ^{13}C NMR showed a progressive increase in its amplitude and/or rate by increasing polyurethane concentrations, indicating that segmental mixing at the phase interface prevails at the microscopic level regardless of the changes of the macroscopic domain. Second, an apparent correlation between the ^{13}C NMR line widths of the terminal carbons from polyurethane, the loss tangent, and the ultimate elongation of the polymers was observed at ambient temperature. This suggests that part of the energy dissipation detected by the loss tangent is due to the motion of terminal carbons. Solid-state high-resolution ^{13}C NMR measurements can thus complement other mechanical and morphological studies to provide detailed information on the two-phase interaction of SINs.

Introduction

Interpenetration polymer networks[1] are a class of polymer blend where one polymeric network is synthesized in the presence of another previously established network. A simultaneous interpenetrating network, SIN, is formed when the polymerizations are carried out simultaneously by independent and noninterfering routes.[2,3] The existence of such interpenetrating network structures provides a novel way to control the mechanical behavior[4] and phase properties[5] of the two-phase materials. Because of the multiple chemical compositions and synthetic details involved in the formation of SINs, polymers with very different mechanical behavior can be made.[6–9] Of the features that control the behavior of blends, microphase structures[10] and molecular interactions[11,12] between phases are of greatest interest to us. It is believed that the physical interactions between phases are equally as important as the chemical cross-links between the constituent components for determining the mechanical properties of the two coexisting phases.[1,3]

Castor oil–polyurethane (COPU) and polystyrene (PS) SINs have been reported some time ago to have a complex two-phase morphology.[5] Mechanical properties of such COPU/PS two-phase systems[13,14] have been shown to be related to the degree of phase continuity and inversion. Most of the phase properties were explored by techniques such as dynamic mechanical analysis, optical microscopy, or modulus measurements. These techniques have provided us with useful information concerning the domain structures at the macroscopic level. It remained to be established at the molecular level[15,16] how the interactions between individual components at the phase interface could affect mechanical properties of interpenetrating networks. This information is important for understanding the mechanism of physical and mechanical behaviors of the related polymers.[12] Up to now, only small-angle X-ray scattering and small-angle neutron scattering have provided us with quantitative information about the interfacial surface properties of SINs.[10]

The purpose of this investigation is to study the molecular properties of the two-phase systems of SINs. We first investigated the phase properties of SINs by using traditional approaches such as modulus measurement, dynamic mechanical analysis, and electron microscopic studies. Solid-state high-resolution ^{13}C NMR[16,17] was then applied to reveal the microscopic molecular interactions for the samples with known phase and mechanical properties. It will be shown that PU is entangling into the PS network regardless of the macroscopic domains of the polymers. In addition, a possible correlation between the mobility of the terminal hydrocarbon group, the loss tangent, and the toughness of SINs will be discussed.

Experimental Section

Materials and Synthesis. The synthesis of a series of SINs with desired weight percentage mixtures of castor oil–polyurethane (COPU) and polystyrene (PS) was done by a modified method of Devia et al.[14] Briefly, castor oil (Fisher Co.) activated by dibutyltin dilaurate was reacted with dimeryl diisocyanate (Henkel Co.) to form castor oil–polyurethane (COPU) prepolymer with NCO/OH ratios of 2.2. Styrene monomer (Osaka Co.) with its free radical initiator (benzoyl peroxide) was mixed with COPU prepolymer and castor oil at NCO/OH ratios of 0.95. SIN samples prepared by curing the full mixed resin at 30 °C for 24 h and 60 °C for 24 h (COPU/PS ratios of 100/0, 89/11, 68/32, 50/50, 35/65, 15/85, and 0/100) were used for modulus, mechanical, morphological, and NMR investigations.

Characterization. Tensile strength, elongation, and Young's modulus of materials were measured by the use of an Instron

* To whom correspondence should be addressed.

0024-9297/91/2224-4605$02.50/0

1137 tester at room temperature. The specimens were prepared and tested at a strain rate of 5 cm/min according to the ASTM D638 Type IV method. The results are reported as an average of three specimens for each sample. Domain structures were then analyzed by modulus–composition data. The relationship between volume fraction of one continuous domain phase and tensile Young's modulus has been given by Kerner[18] for spheres dispersed in a continuous matrix. Depending on whether COPU or PS forms a continuous phase, a theoretical lower bound and upper bound modulus can be obtained according to the Kerner equation:

$$E/E_m = [\gamma(1 - V_i)E_m + \beta(\alpha + V_i)E_i]/[(1 + \alpha V_i)E_m + \alpha\beta(1 - V_i)E_i] \quad (1)$$

where $\alpha = 2(4 - 5\nu_m)/(7 - 5\nu_m)$, $\beta = (1 + \nu_m)/(1 + \nu_i)$, $\gamma = (1 + \nu)/(1 + \nu_m)$, $\nu = V_m\nu_m + V_i\nu_i$, E is Young's modulus, V is the volume fractions, ν is Poisson's ratio, and the subscripts i and m represent respectively the dispersive and continuous phase for the two-phase systems. Poisson ratios for COPU and PS have been assumed to be 0.5 and 0.35, respectively, in the present study. Densities used for volume fraction calculation were determined by methods of density column and autopycnometer (Micromeritics Auto Pycnometer Type 1320). Densities for pure COPU and PS polymers were found to be 0.95 and 1.053 g/cm^3, respectively.

To reveal the viscoelastic and phase properties of SINs, dynamic mechanical analyses were performed by using a Rheometrics dynamic spectrometer (Model RDS-7700). The temperature range employed was from −100 to 150 °C with an increment of 3 °C and a 1-min soaking time between each measurement. A frequency of 75 Hz was employed. Scanning electron microscopy (Hitachi S-570) was also applied to study the morphology of the ruptured surface in order to understand the domain structures of SINs. Samples of 3 mm × 2 cm × 1 cm were tensile stressed to rupture at room temperature and directly observed under SEM after coating with gold particles.

Nuclear Magnetic Resonance Experiments. Solid-state high-resolution ^{13}C NMR experiments were performed on a Brüker MSL-200 NMR spectrometer equipped with a 4.7-T superconducting magnet. The operating frequencies were 200.13 and 50.33 MHz for ^1H and ^{13}C nuclei, respectively. Carbon spectra were obtained by cross-polarization with magic angle spinning[17] at approximately 2 kHz, depending on the sample packing conditions. Samples were prepared by cutting the blend into 1–2-mm particles for ease of sample spinning. Cross-polarization was established by using a single-contact Hartmann–Hahn match at approximately 40-kHz rf field. The contact times were varied from 0.1 to 32 ms. Rotating frame proton relaxation times,[16] $T_{1\rho}$, were determined by fitting intensities as a function of contact times according to

$$I(t_c) = I(0)e^{-t_c/T_{1\rho}}[1 - e^{-t_c(1/T_{HC}-1/T_{1\rho})}] \quad (2)$$

where t_c is the time of dipolar contact, T_{HC} is the cross-polarization time constant, and $T_{1\rho}$ is the spin–lattice relaxation time in the rotating frame of the proton reservoir. Chemical shifts were referenced to an external standard of tetramethylsilane (TMS).

Results

Sample Characterization. Figure 1 shows representative tensile stress–strain curves of SINs at indicated COPU/PS ratios. It can be seen that the elastomer to show the highest measurable elongation, i.e., maximum extensibility, is the sample with 50 wt % COPU. To study the phase properties of SINs, modulus–composition relationships were plotted in Figure 2. The tensile Young's moduli for samples with COPU contents higher than 50% were found to be similar to that of pure COPU. On the other hand, samples with COPU/PS ratios of 11/89 showed high Young's moduli with values close to that of pure PS. Quantitative analysis on the modulus–composition data of Figure 2 by Kerner's model suggests that a phase inversion occurs between 20% and 30% COPU. In other words, COPU continuous phase at low PS content has been transformed to PS continuous phase at high PS content.

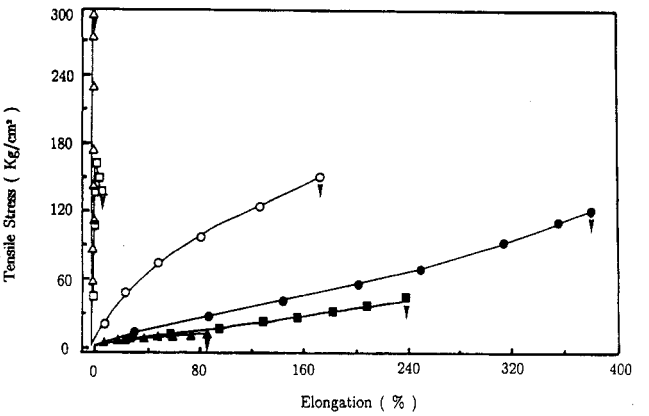

Figure 1. Stress–strain studies on COPU/PS SINs. Arrows indicate the points where ultimate elongation was detected. The six curves represent (from left to right) samples with COPU/PS ratios of 0/100, 15/85, 35/65, 50/50, 68/32, and 89/11, respectively.

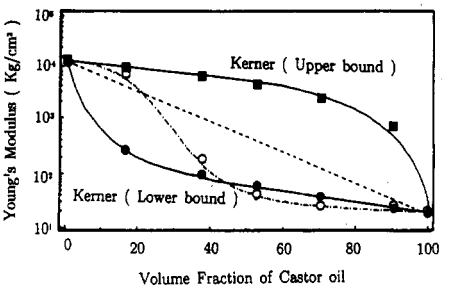

Figure 2. Young's modulus plotted against the volume fraction of COPU and compared with the theoretical Kerner model. Open symbols show the experimental modulus. Close symbols show the theoretical upper bound (squares) and lower bound (circles).

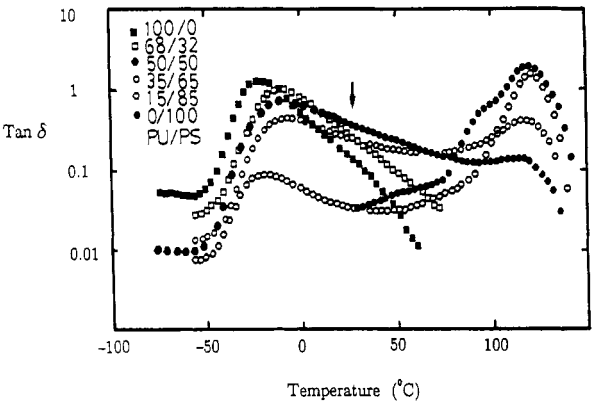

Figure 3. tan δ versus temperature curves for SINs at indicated COPU/PS ratios. The arrow indicates the loss tangent measurements at room temperature.

The extent of mixing of the two phases can be reflected by the dynamic mechanical measurement. Figure 3 shows the representative temperature dependence of the tangent loss, tan δ, for the studied SINs. Two points can be seen. First, the glass transition temperatures, T_gs, of the COPU and PS phases detected by viscoelastic measurements at 75 Hz were slightly shifted toward each other by mixing each component in SINs. This may indicate the segmental mixing for the two separate phases. Second, the determined tan δ is largest for the sample with 50 wt % COPU at ambient temperature. As we mentioned before, the same sample also exhibited the highest ultimate elongation at the same temperature.

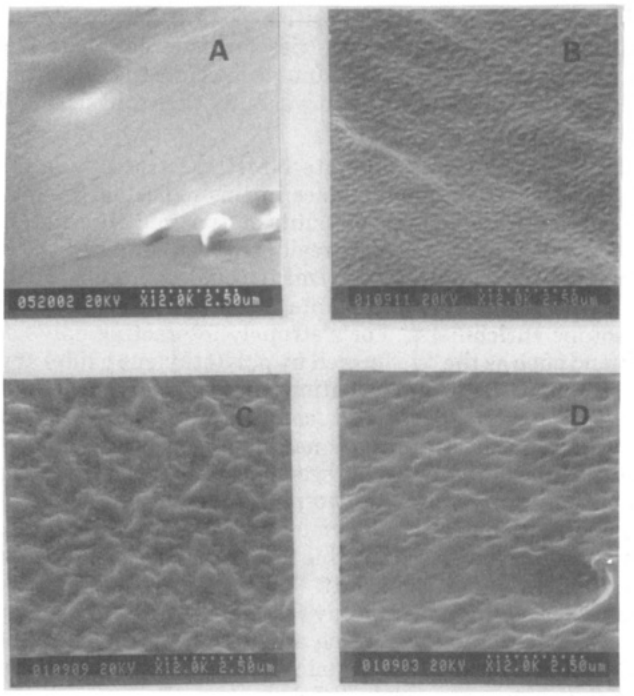

Figure 4. Scanning electron micrograph of the ruptured surface of SINs. The phase inversion process occurred between 20% and 30% COPU as indicated by the transformation of the dispersed separate domain (panel C) into the continuous phase (panel D). Each micrograph represents the ruptured surface obtained from a COPU/PS ratio of (A) 68/32, (B) 50/50, (C) 35/65, and (D) 15/85.

Shown in Figure 4 are the electron micrographs of the replica of the ruptured surface of SINs at indicated COPU and PS ratios. The domain size of the sample with a COPU/PS ratio of 50/50 (panel B) is much smaller than the sample with a COPU/PS ratio of 35/65 (panel C). In addition, these dispersed domains have been transformed into a continuous one at a COPU/PS ratio of 15/85 (panel D). The morphology of the ruptured sample with high COPU content (panel A) is different from that with high PS content (panel D). This is consistent with the modulus–composition results (Figure 2) that a phase inversion occurs between 20% and 30% COPU.

NMR Studies. To understand the aforementioned phase structures and mechanical behaviors at the molecular level, we carried out solid-state high-resolution ^{13}C NMR studies. Figure 5 shows representative ^{13}C NMR spectra of SINs with a COPU/PS ratio of 50/50. In the same figure, liquid-state high-resolution ^{13}C NMR spectra of both styrene monomer and castor oil were included for comparison. Several well-resolved peaks can be assigned. Polystyrene consists of three lines: a quaternary carbon resonance (δ_c 146), a combination aromatic carbon resonance (δ_c 128), and a main-chain aliphatic carbon resonance (δ_c 41). Spectra of SINs show several extra peaks in the methylene region (δ_c from 10 to 30). Magic angle spinning produced a spinning sideband of PS resonances due to the strong dipolar and chemical shift interaction of aromatic carbons.[11]

The residual line width of the high-resolution resonance peak after magic angle spinning is partly due to the inhomogeneous dipolar interaction from neighboring protons. Although the residual line width would broaden the NMR signals of the studied samples and prevent us from detecting chemically interacting functional group at cross-links, it still allows us to study physical interactions between individual components. Figures 6 and 7 show

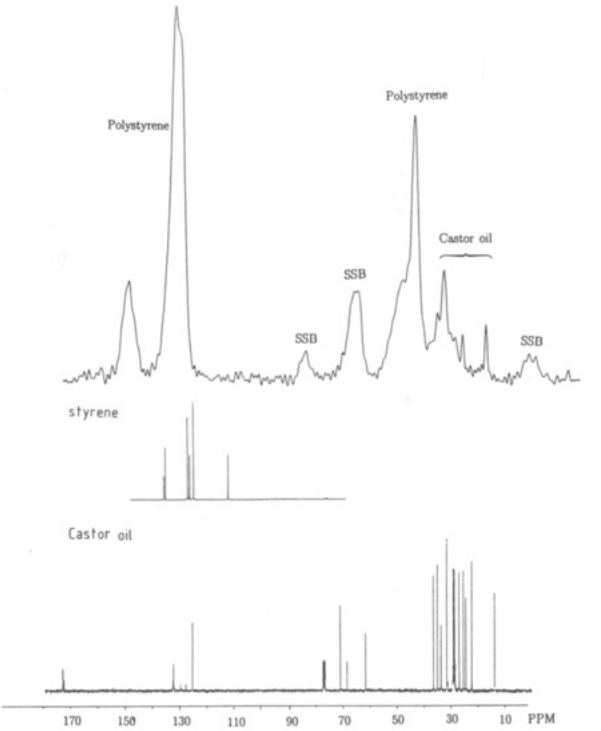

Figure 5. ^{13}C NMR spectra for SINs with a COPU/PS ratio of 50/50 obtained by the cross-polarization/magic angle spinning technique. Liquid-state ^{13}C NMR spectra of the styrene monomer and castor oil were included for comparison. Chemical shifts were relative to external TMS.

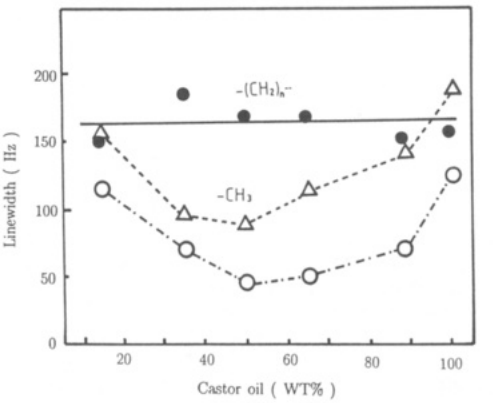

Figure 6. ^{13}C NMR line width for the representative COPU signals plotted against PU content. Line widths at half-height were obtained for peaks at 30.2 ppm (●), 26.3 ppm (○), and 14.9 ppm (△).

the peak width at half-height as a function of chemical compositions for ^{13}C signals from PU and PS, respectively. It can be seen that some signals revealed significant changes in the line width by changing the COPU/PS ratio, whereas other kept their line width relatively constant. The differential line-broadening effect suggests that the relative change of the line width must be due to the change of the local motional mode of the studied carbon residues at either its amplitude or its frequency. Specifically, the line width for the aromatic ring of PS is seen to decrease monotonically with increasing COPU content (Figure 7). In contrast, the line width for the terminal carbons of COPU shows a minimum at approximately 50% COPU (Figure 6). This suggests a possible relationship between the terminal carbon mobility and the mechanical properties of SINs (see Figures 1 and 3). The progressive decrease of the NMR line width for certain aromatic ring signals is most interesting since we have shown by other macroscopic techniques that there were dispersed domains in

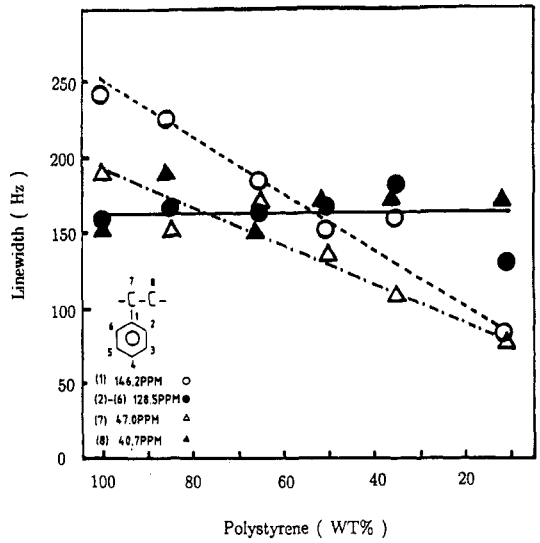

Figure 7. ^{13}C NMR line width for the representative PS signals plotted against PS content.

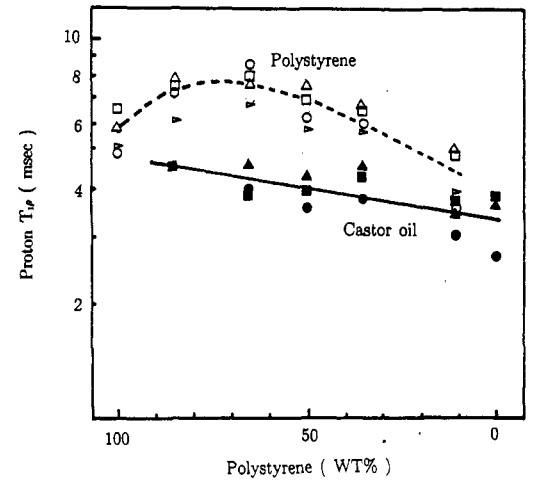

Figure 8. Proton spin–lattice relaxation time in the rotating frame, $T_{1\rho}$, plotted as a function of PS content. Closed symbols are $T_{1\rho}$ values of COPU and open symbols are those of PS. Different symbols represent data from different ^{13}C NMR signals: 26.3 ppm (●), 30.2 ppm (■), 32.7 ppm (▲), 40.7 ppm (○), 45.0 ppm (▷), 128.5 ppm (△), and 146.2 ppm (□). Their similarity suggests that spin diffusion is the dominating relaxation mechanism.

SINs and a phase inversion occurred at 20–30% COPU. We will discuss this point in the Discussion section.

Finally, proton spin–lattice relaxation times in the rotating frame, $T_{1\rho}$, were measured. $T_{1\rho}$ values of COPU were detected to be similar for all proton reservoirs connected to carbon nuclei (Figure 8) with the exception of terminal carbons (data not shown). $T_{1\rho}$ values of PS, which were slightly larger than those of COPU, were also detected to be similar for all carbon signals. This suggests that intrachain proton–proton spin diffusion dominates the ^1H $T_{1\rho}$ relaxation mechanism. Interestingly, as shown in Figure 8, $T_{1\rho}$ increased linearly by increasing the PS content but decreased again at a higher PS ratio. The maximum of the detected $T_{1\rho}$ value was found to be between COPU/PS ratio of 35/65 and 15/85, corresponding to the point where phase inversion (Figure 2) occurred.

Discussion

For the past decade, many studies of interpenetrating polymer network have been carried out on their morphology and mechanical and thermal behavior. Since the formation of SINs is sensitive to synthetic details,[2] different mechanical properties for different materials appeared. Hence, it is important to look into the properties at the molecular level when we study their physical and mechanical behavior.

High-resolution solid-state NMR spectroscopy is the analytical technique of choice in this molecular investigation. Although large amounts of dynamic information on polymer networks has previously been obtained by ^2H NMR,[20] cross-polarization/magic angle spinning (CP/MAS) ^{13}C NMR has an advantage in its sensitivity without isotope enrichment. For a strongly interacting polymer blend such as the one formed by poly(ethylene oxide) and resorcinol, large parturbations in ^{13}C NMR isotropic chemical shift parameter can be detected.[19] It was suggested that conformational, hydrogen bond, molecular complexation, or packing geometry changes might occur concomitantly with the two-phase mixing process. For the interpenetrating polymer networks such as SINs studied here, we were not able to detect significant change in the NMR chemical shift. This suggests that the two interacting components only associate with each other via physical interactions, which are not strong enough to be detected by the NMR chemical shift. This is consistent with the current model of SINs.[1] Nevertheless, we could detect significant changes in the NMR line width as a function of composition (Figures 6 and 7). In the following, we will use this information to shed some light on the phase and mechanical properties of SINs at the molecular level.

Polystyrene Mobility, Spin Diffusion, and Microphase Structure. Molecular motions of PS have been studied previously by both solid-state ^{13}C NMR[11,16] and ^2H NMR.[20] It has been proposed that PS shows restricted phenyl rotation with a sizable average jump angle. The amplitude and frequency of this motion vary from one substituted PS to another. Since the line widths of the quatenary carbon and its covalent bound main-chain carbon were reduced progressively by increasing COPU concentrations (Figure 6), this suggests strongly that the phenyl rotation is also present in SINs and can be affected by the presence of COPU. It has been proposed that flipping of a ring demands some distortion of the polymer lattice. The intertwining of COPU and PS networks would provide a mechanism for the breaking of the polymer lattice and thus enhance the amplitude of its phenyl rotation. The important observation from this study is that the phenyl rotation depends only on the relative ratio of COPU and PS but not on the variation of the macroscopic phase domain. PU must entangle into the PS network at the phase interface to perturb the aromatic phenyl rotation regardless of the macroscopic structures.

A standard CP/MAS ^{13}C NMR experiments as a function of contact time allows us to determine the ^1H $T_{1\rho}$. Proton $T_{1\rho}$'s are sensitive to spatially dependent proton–proton spin diffusion in polymers. As clearly demonstrated in Figure 8, spin diffusion is present in SINs from COPU/PS, since all the ^1H $T_{1\rho}$ values were similar for the proton signals from the same component, i.e., COPU or PS. The spin diffusion, however, did not pass across between the two components, for their respective $T_{1\rho}$'s were detected to be different. Coincidently, the largest ^1H $T_{1\rho}$ values lie in SINS with COPU/PS ratios between 15/85 and 35/65. Within this compositional range, mechanical and electron microscopic data also showed the occurrence of phase inversion. In the spin diffusion process, the maximum diffusive path length L is approximately expressed as $L \sim (6D\tau_{sd})^{1/2}$, where D is the spin

diffusion coefficient and τ_{sd} is the characteristic time for diffusion.[12] Hence, ^1H $T_{1\rho}$ experiments provide a measure of the dimension of the microdomains involved in the process. If $T_{1\rho}$ values are taken as approximately 10^{-1} s and typical values of D as 10^{-12} cm^2/s^{-1}, the dimension of L can be roughly estimated as 100 Å. This is 2–3 orders magnitude smaller than the domains observed by microscopic methods (typically in the range 0.1–1 μm). This indicates the presence of a large heterogeneity in the microstructure of the COPU/PS network. Interestingly, the distances of heterogeneity L_c of polyurethane–poly(urethane acrylate) SINs estimated by small-angle X-ray scattering were found to be in the range 550–123 Å.[10] Our NMR results are thus comparable to small-angle scattering results.

Based on the information obtained so far, we wish to discuss a model of microphase structures in the macroscopic domain of SINs. The microscopic packing arrangement of the interpenetrating polymer network at the molecular level has not been addressed before. According to our scanning electron microscopic studies of the ruptured surface and previous optical micrographic and transmission electron microscopic investigations of the stained thin-section SINs, distinct macroscopic domains with sizes from 0.1 to 10 μm are present, depending on their compositional ratio. Inside this macroscopic domain, the microphase structures of the two-phase system are quite complex and show a high degree of heterogeneity. First, COPU must entangle into the PS network, as evidenced by the phenyl rotation of PS side chain introduced by increasing PU concentrations. Second, the PS or PU phase should be present with a size of approximately 100 Å, as shown by the proton NMR spin diffusion data, in contrast to the micrometer size of the macroscopic domain detected by most microscopic measurements. The segmental mixing of the two components was also detected by the dynamic mechanical measurements (Figure 3), where the T_gs of each component were found to shift toward each other. The degree of mixing between the two components, however, is not homogeneous, since each T_g point was only slightly affected by the mixing process and remained resolvable as an independent melting peak. According to the data available to us now, we are not able to suggest how the mutual entanglement of PU and PS networks can accommodate keeping the microphase domain relatively intact. Future investigations using other techniques such as detailed relaxation analysis of ^1H, ^2H, or ^{13}C NMR might give us more information on the molecular interaction of the two-phase systems. In conclusion, the packing arrangement of the interpenetrating polymer network at the molecular level is quite complex, but it is clear that the two phases must interact at the microscopic level inside the macroscopic domain.

Ultimate Elongation, Loss Tangent, and Hydrocarbon Chain Mobility. As mentioned in the Results section, the SIN sample with 50% COPU showed optimum properties in three quite different physical studies; i.e., ultimate elongation measured by the stress–strain experiments (Figure 1), tan δ measured by the dynamic spectrometer at 75 Hz (Figure 3), and the line width of terminal hydrocarbon signals measured by ^{13}C NMR (Figure 6). A discussion on the underlined molecular mechanism that accounts for the apparent correlation of the data obtained by these three measurements should be useful in understanding the structure–property relationship in SINs.

It is well-known that the loss tangent, tan δ, is a measure of the energy dissipation. The energy dissipation of a polymer depends on the investigated frequency. Mechanistically, it is usually associated with molecular motion of certain structural groups in the materials.[21] The apparent consistency between data obtained from dynamic mechanical measurements and NMR line-width measurement suggests that part of the energy dissipation detected by tan δ is from the molecular motion of the hydrocarbon terminal group of COPU. The molecular mobility of each component in polymers can in principle be directly estimated by the measurement of the spin–spin relaxation time (T_2). Since the peak width at half-height, $(\delta\nu)_{1/2}$, is known to be related to the apparent T_2 by $(\delta\nu)_{1/2} = (\pi T_2)^{-1}$, a detected change of line width in the ^{13}C NMR signals can represent changes of segmental motion. It should be mentioned that the line widths of main polymethylene signals remain approximately constant (~170 Hz). Therefore, variation of the line width for a terminal fatty acyl carbon cannot be due to the experimental conditions applied on each individual sample.

The possible relationship of ultimate elongation, i.e., maximum extensibility, to the molecular motion of the hydrocarbon chain and to the energy dissipation of polymers is less clear. The area under the stress–elongation curve as shown in Figure 1 represents the rupture energy and, thus, the toughness of the studied SINs. If the dissipated energy is highest for the 50% COPU sample, it is possible that the same sample exhibits the highest toughness against rupture. This is consistent with the observation that a 50% COPU sample showed maximum extensibility. It should be pointed out that the factors affecting the ultimate properties are different from the factors affecting the elasticity of the elastomers. According to the rubber elasticity theory, the later process is reversible and the conformational flexibility of the long chain between the hard domains or cross-links is mainly responsible for the elasticity. In contrast, rupture should occur at the "weakest link". As judged from the morphology of the ruptured surface, it probably occurred at the interfacial region of the detected macroscopic domain. It will be of future interest to investigate how the structure responsible for the weakest link could be reflected in the mobility of terminal hydrocarbon group.

In summary, we have applied the CP/MAS ^{13}C NMR technique, in combination with other mechanical and morphological methods, to investigate the details of the microphase structures of SINs at the molecular level. Evidence is provided to indicate the formation of chain entanglement between the constituent polymers regardless of the detected phase separation and inversion in the studied materials. Since solid-state high-resolution NMR can now be used in a routine manner, it can thus complement other macroscopic techniques to reveal the details of the two-phase interactions in polymer blends.

References and Notes

(1) Sperling, L. H. *CHEMTECH* **1988**, *Feb*, 104.
(2) Devia, N.; Manson, J. A.; Sperling, L. H.; Conde, A. *Macromolecules* **1979**, *12*, 360.
(3) Klempner, D.; Frisch, K. C.; Xiao, X. H.; Frisch, H. L. *Polym. Eng. Sci.* **1985**, *25*, 488.
(4) Morin, A.; Djomo, H.; Meyer, G. C. *Polym. Eng. Sci.* **1983**, *23*, 394.
(5) Jordhamo, G. M.; Manson, J. A.; Sperling, L. H. *Polym. Eng. Sci.* **1986**, *26*, 517.
(6) Sperling, L. H. *Polym. Eng. Sci.* **1985**, *25*, 517.
(7) Xue, S.; Zhang, Z.; Ying, S. *Polymer* **1989**, *30*, 1269.
(8) Xiao, H.; Ping, Z. H.; Xic, J. W.; Yu, T. Y. *J. Polym. Sci., Polym. Chem.* **1990**, *28*, 585.
(9) Patel, P.; Suthar, B. *Polymer* **1990**, *31*, 339.

(10) Sperling, L. H. *Encyclopedia of Polymer Science and Engineering*; Kroschwitz, Ed.; Wiley: New York, 1987; Vol. 9, p 760.
(11) Schaefer, J.; Sefcik, M. D.; Stejskal, E. O.; Mckay, R. A.; Dixon, W. T.; Cais, R. E. *Macromolecules* **1984**, *17*, 1107.
(12) Fukumori, K.; Kurauchi, T.; Kamigaito, O. *J. Appl. Polym. Sci.* **1989**, *38*, 1313.
(13) Yenwo, G. M.; Sperling, L. H.; Pulido, J.; Manson, J. A.; Conde, A. *Polym. Eng. Sci.* **1977**, *17*, 251.
(14) Devia, N.; Manson, J. A.; Sperling, L. H.; Conde, A. *Polym. Eng. Sci.* **1978**, *18*, 200.
(15) Ebdon, J. R.; Hourston, D. J.; Klein, P. G. *Polymer* **1984**, *25*, 1633.
(16) Schaefer, J.; Sefcik, M. D.; Stejskal, E. O.; Mckay, R. A. *Macromolecules* **1981**, *14*, 188.
(17) Schaefer, J.; Stejskal, E. O. *J. Am. Chem. Soc.* **1976**, *98*, 1031.
(18) Kerner, E. H. *Proc. Phys. Soc. London* **1956**, *B69*, 808.
(19) Belfiore, L. A.; Lutz, T. J.; Cheng, C.; Bronnimann, C. E. *J. Polym. Sci., Polym. Phys. Ed.* **1990**, *28*, 1261.
(20) Spiess, H. W. *Colloid Polym. Sci* **1983**, *261*, 193.
(21) Nielsen, L. E. In *Mechanical properties of polymers and composites*, Marcel Dekker, Inc.: New York, 1974; Vol. 1, Chapter 4.